Published for SISSA by Springer

Received: December 30, 2013
Accepted: December 31, 2013
Published: January 29, 2014

Erratum: Simplified models for dark matter interacting with quarks

Anthony DiFranzo,[a] **Keiko I. Nagao,**[b,c] **Arvind Rajaraman**[a] **and Tim M.P. Tait**[a]

[a] *Department of Physics and Astronomy, University of California, 4129 Frederick Reines Hall, Irvine, CA 92697-4575, U.S.A.*
[b] *Theory Center, KEK, 1-1 Oho, Tsukuba, Ibaraki 305-0801, Japan*
[c] *Department of Engineering Science, Niihama National College of Technology, 7-1 Yagumo, Niihama, Ehime 792-8580, Japan*

E-mail: adifranz@uci.edu, nagao@sci.niihama-nct.ac.jp, arajaram@uci.edu, ttait@uci.edu

Erratum to: JHEP11(2013)014

ArXiv ePrint: 1308.2679

JHEP01(2014)162

A term was erroneously dropped during the derivation of the direct detection cross section calculation. The error is first seen in eq. (3.2) and is carried through all of the equations in section 3.2. Equations (3.2)–(3.14) should be replaced as follows:

$$\mathcal{M} \approx (-ig_{DM})^2(\bar{\chi}P_R u)\frac{-i}{M_{\tilde{u}}^2 - M_\chi^2}(\bar{u}P_L\chi) \tag{3.2}$$

$$\mathcal{M} = \frac{ig_{DM}^2}{M_{\tilde{u}}^2 - M_\chi^2}\frac{1}{2}(\bar{\chi}\gamma^\mu P_L\chi)(\bar{u}\gamma_\mu P_R u) \tag{3.3}$$

$$= \frac{ig_{DM}^2}{M_{\tilde{u}}^2 - M_\chi^2}\frac{1}{8}\left[(\bar{\chi}\gamma^\mu\chi)(\bar{u}\gamma_\mu u) - \left(\bar{\chi}\gamma^\mu\gamma^5\chi\right)(\bar{u}\gamma_\mu\gamma_5 u)\right.$$
$$\left. + \left(\bar{\chi}\gamma^\mu\gamma^5\chi\right)(\bar{u}\gamma_\mu u) - (\bar{\chi}\gamma^\mu\chi)(\bar{u}\gamma_\mu\gamma_5 u)\right] \tag{3.4}$$

$$\approx \frac{ig_{DM}^2}{M_{\tilde{u}}^2 - M_\chi^2}\frac{1}{8}\left[(\bar{\chi}\gamma^\mu\chi)(\bar{u}\gamma_\mu u) - \left(\bar{\chi}\gamma^\mu\gamma^5\chi\right)(\bar{u}\gamma_\mu\gamma_5 u)\right]. \tag{3.5}$$

doi:10.1007/JHEP01(2014)162

For Dirac dark matter:

$$\sigma_{SI}^{u_R} = \frac{1}{64\pi} \frac{M_N^2 M_\chi^2}{\left(M_N + M_\chi\right)^2} \frac{g_{DM}^4}{\left(M_{\tilde{u}}^2 - M_\chi^2\right)^2} \left(1 + \frac{Z}{A}\right)^2 \tag{3.6}$$

$$\sigma_{SD}^{u_R} = \frac{3}{64\pi} \frac{M_N^2 M_\chi^2}{\left(M_N + M_\chi\right)^2} \frac{g_{DM}^4}{\left(M_{\tilde{u}}^2 - M_\chi^2\right)^2} (\Delta u^N)^2 \tag{3.7}$$

$$\sigma_{SI}^{d_R} = \frac{1}{64\pi} \frac{M_N^2 M_\chi^2}{\left(M_N + M_\chi\right)^2} \frac{g_{DM}^4}{\left(M_{\tilde{d}}^2 - M_\chi^2\right)^2} \left(2 - \frac{Z}{A}\right)^2 \tag{3.8}$$

$$\sigma_{SD}^{d_R} = \frac{3}{64\pi} \frac{M_N^2 M_\chi^2}{\left(M_N + M_\chi\right)^2} \frac{g_{DM}^4}{\left(M_{\tilde{d}}^2 - M_\chi^2\right)^2} \left(\Delta d^N + \Delta s^N\right)^2 \tag{3.9}$$

$$\sigma_{SI}^{q_L} = \frac{9}{64\pi} \frac{M_N^2 M_\chi^2}{\left(M_N + M_\chi\right)^2} \frac{g_{DM}^4}{\left(M_{\tilde{q}}^2 - M_\chi^2\right)^2} \tag{3.10}$$

$$\sigma_{SD}^{q_L} = \frac{3}{64\pi} \frac{M_N^2 M_\chi^2}{\left(M_N + M_\chi\right)^2} \frac{g_{DM}^4}{\left(M_{\tilde{q}}^2 - M_\chi^2\right)^2} \left(\Delta u^N + \Delta d^N + \Delta s^N\right)^2 . \tag{3.11}$$

For Majorana dark matter:

$$\sigma_{SD}^{u_R} = \frac{3}{16\pi} \frac{M_N^2 M_\chi^2}{\left(M_N + M_\chi\right)^2} \frac{g_{DM}^4}{\left(M_{\tilde{d}}^2 - M_\chi^2\right)^2} \left(\Delta u^N\right)^2 \tag{3.12}$$

$$\sigma_{SD}^{d_R} = \frac{3}{16\pi} \frac{M_N^2 M_\chi^2}{\left(M_N + M_\chi\right)^2} \frac{g_{DM}^4}{\left(M_{\tilde{d}}^2 - M_\chi^2\right)^2} \left(\Delta d^N + \Delta s^N\right)^2 \tag{3.13}$$

$$\sigma_{SD}^{q_L} = \frac{3}{16\pi} \frac{M_N^2 M_\chi^2}{\left(M_N + M_\chi\right)^2} \frac{g_{DM}^4}{\left(M_{\tilde{d}}^2 - M_\chi^2\right)^2} \left(\Delta u^N + \Delta d^N + \Delta s^N\right)^2 . \tag{3.14}$$

This change also propagates to the figures in the paper. For low dark matter mass little changes, however at higher masses deviations are seen. The figures in this erratum should replace those in the original paper. Thus, for accuracy the last paragraph on page 6 should now read, "...we observe the expected behavior where the curves of constant g_{DM} go like $\left(M_\chi^2 - M_{\tilde{q}}^2\right)^{-2}$, similar to the dependence of the direct detection cross section on the two masses." Despite these alterations, there is no qualitative change in our results and therefore no additional changes are necessary.

JHEP01(2014)162

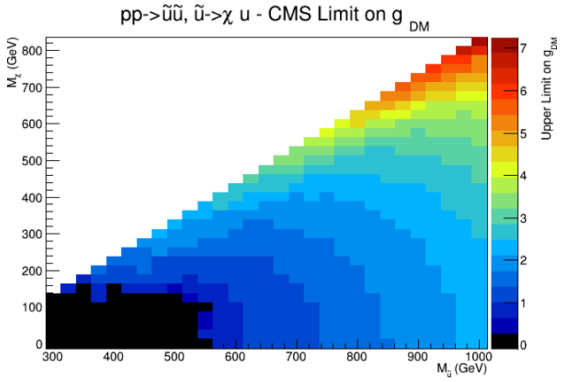

(a)

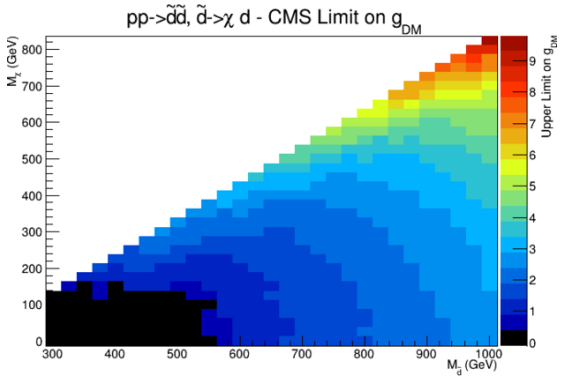

(b)

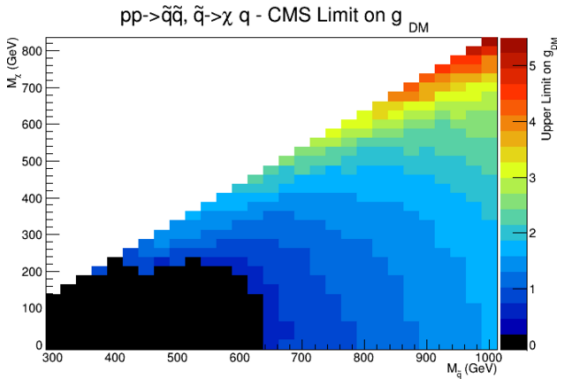

(c)

Figure 1. Bounds on the the coupling g_{DM} for each of the three simplified models with Dirac Dark Matter, from the CMS collider bounds. (a) is the u_R model, (b) the d_R model, and (c) is the q_L model.

JHEP01(2014)162

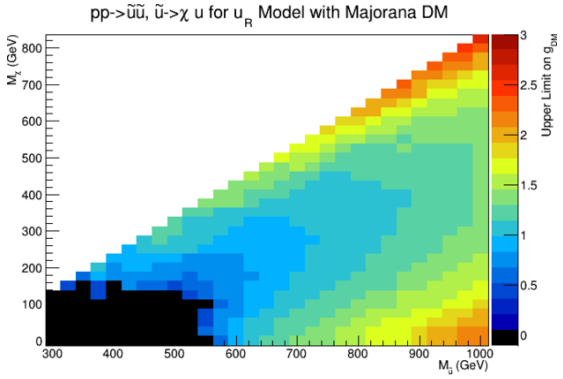

(a)

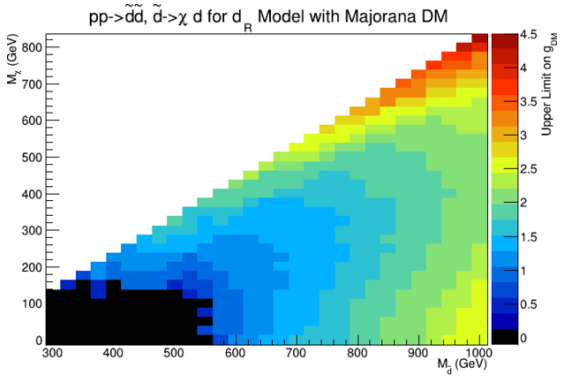

(b)

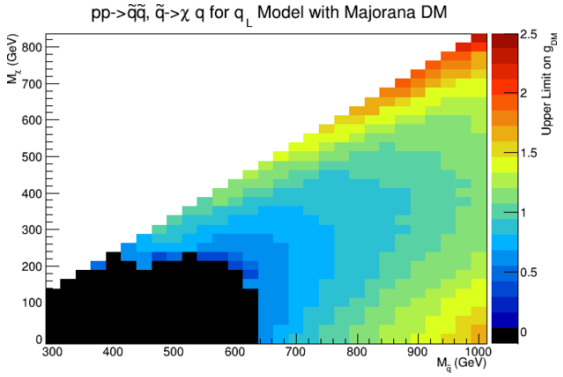

(c)

Figure 2. Bounds on the the coupling g_{DM} for all three models with Majorana Dark Matter, from the CMS collider bounds.

JHEP01(2014)162

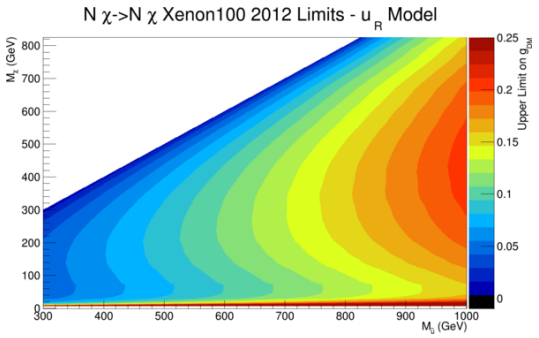

(a)

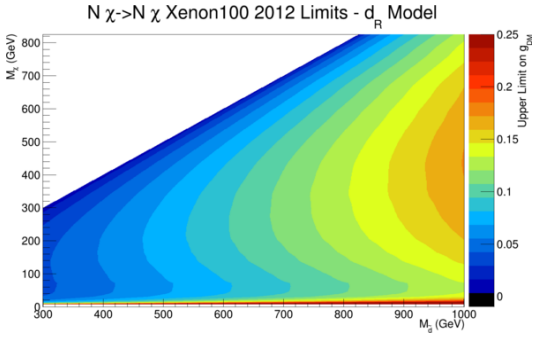

(b)

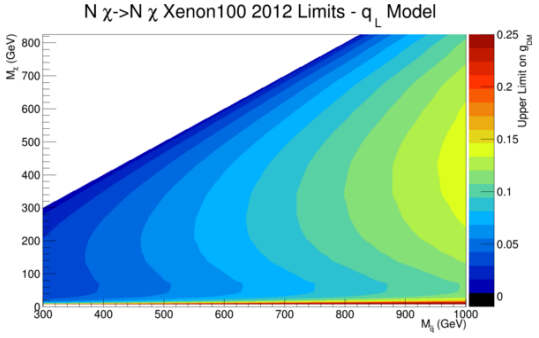

(c)

Figure 3. Bounds on the the coupling g_{DM} for all three models with Dirac Dark Matter, from the spin-independent XENON100 Limits.

JHEP01(2014)162

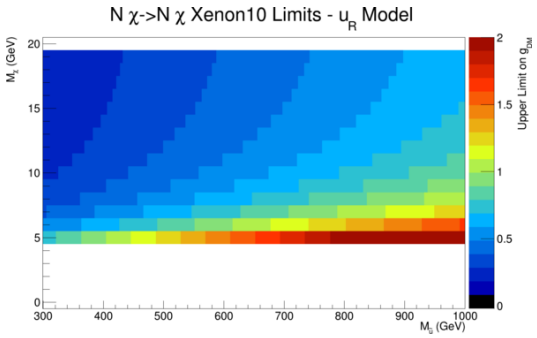

(a)

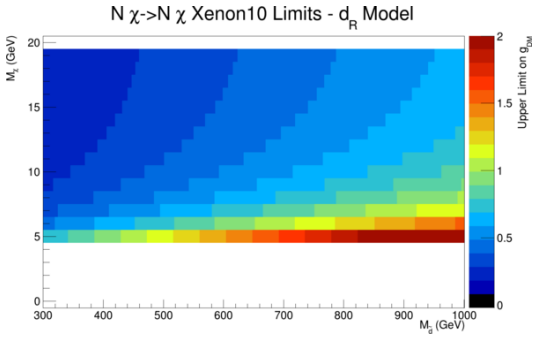

(b)

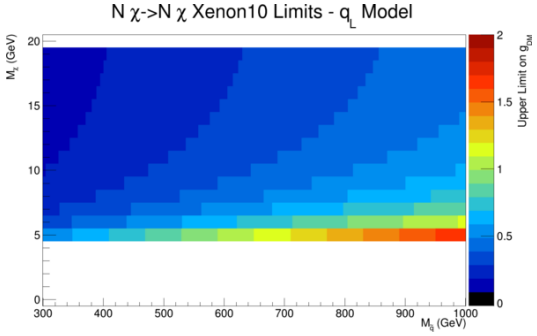

(c)

Figure 4. Dirac Dark Matter bounds on g_{DM} from the spin-indepedent XENON10 Limits.

JHEP01(2014)162

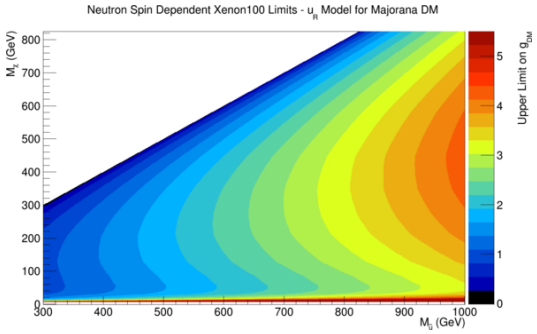

(a)

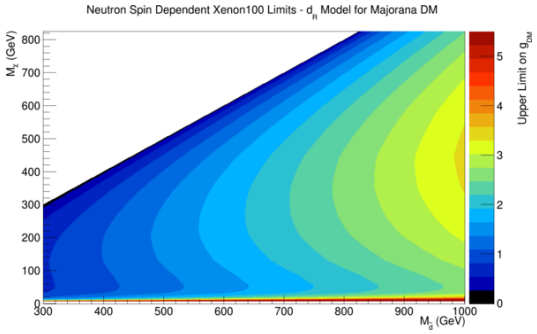

(b)

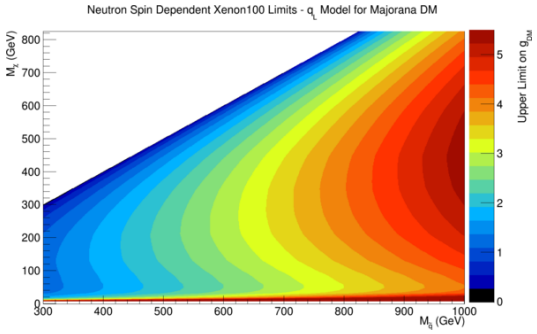

(c)

Figure 5. Bounds on g_{DM} from neutron-WIMP spin-dependent XENON100 Limits on Majorana Dark Matter.

JHEP01(2014)162

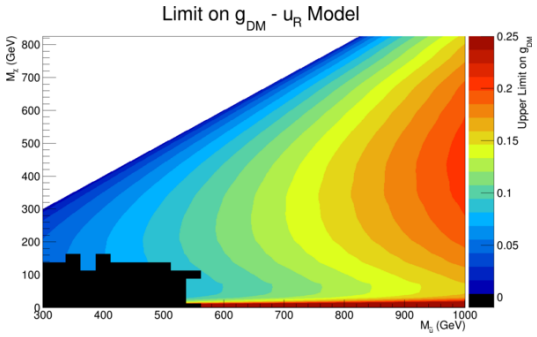

(a)

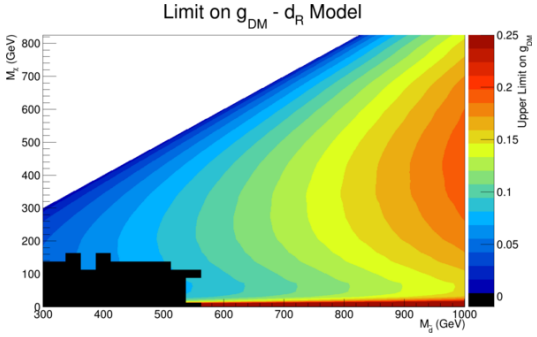

(b)

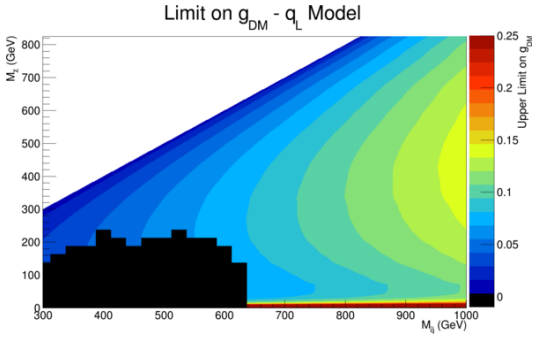

(c)

Figure 6. The combined lowest bounds on g_{DM} from CMS, XENON100, and XENON10 for Dirac Dark Matter.

JHEP01(2014)162

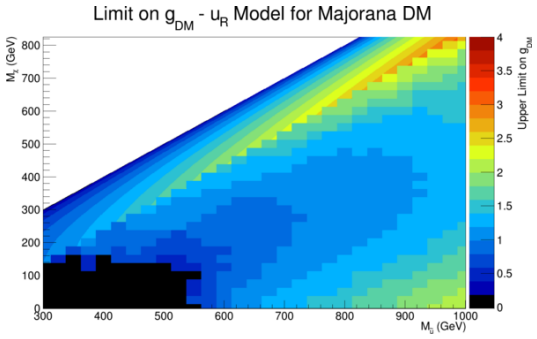

(a)

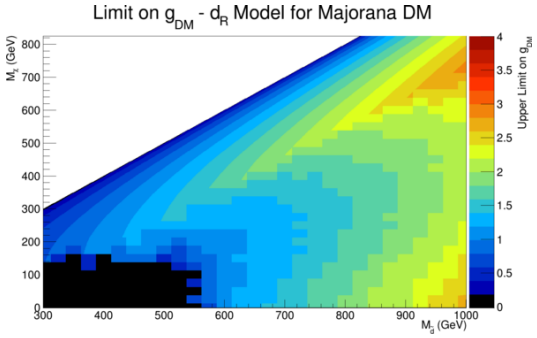

(b)

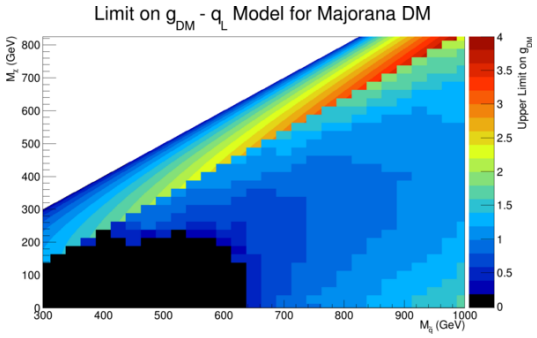

(c)

Figure 7. The combined lowest limit on g_{DM} from CMS and XENON100 for Majorana Dark Matter.

JHEP01(2014)162

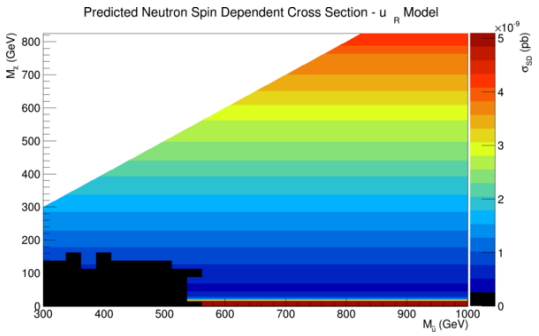

(a)

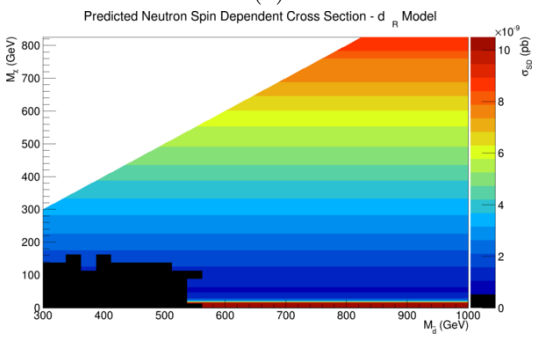

(b)

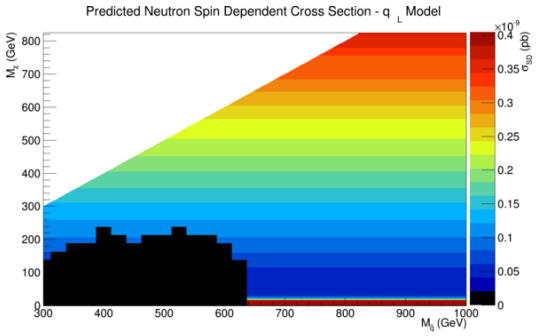

(c)

Figure 8. The predicted maximum spin-dependent neutron-DM cross section from the combined Collider and Direct Detection bounds for Dirac Dark Matter.

JHEP01(2014)162

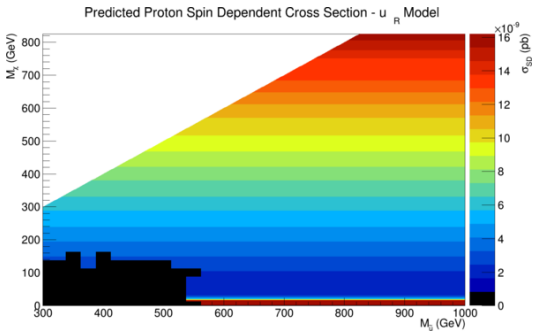

(a)

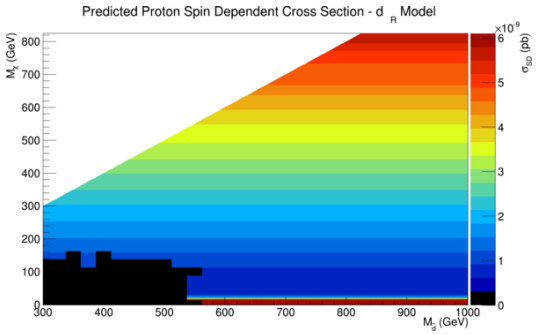

(b)

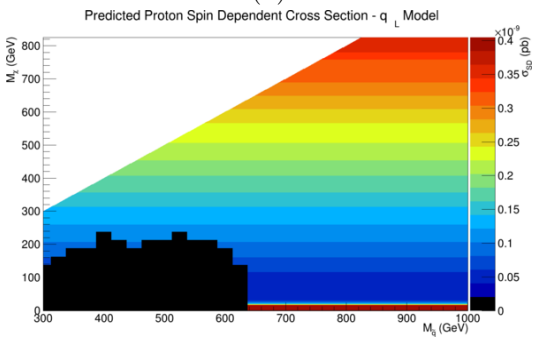

(c)

Figure 9. The predicted maximum spin-dependent proton-DM cross section from the combined Collider and Direct Detection bounds for Dirac Dark Matter.

JHEP01(2014)162

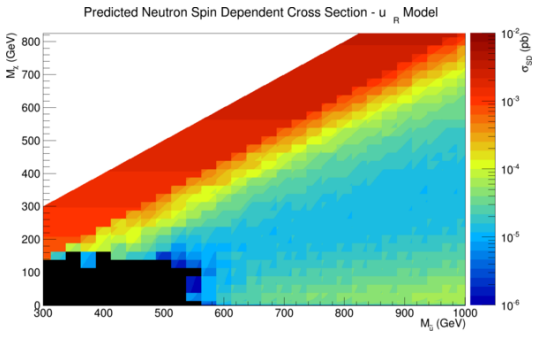

(a)

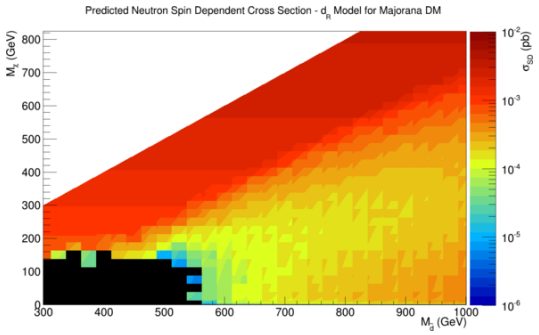

(b)

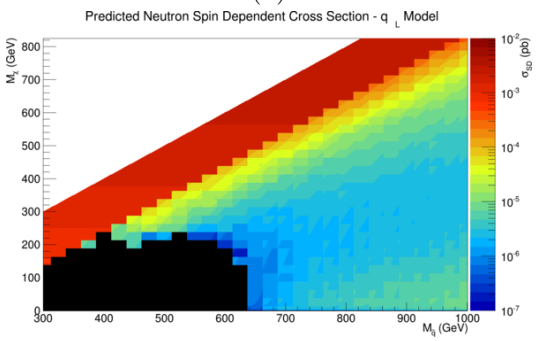

(c)

Figure 10. The predicted maximum spin-dependent neutron-DM cross section from the combined Collider and Direct Detection bounds for Majorana Dark Matter.

JHEP01(2014)162

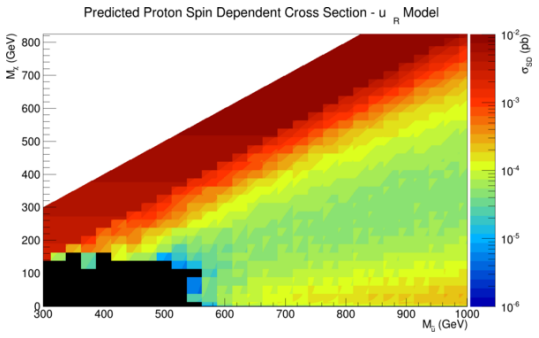

(a)

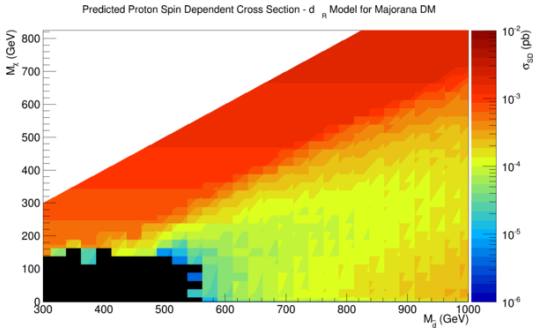

(b)

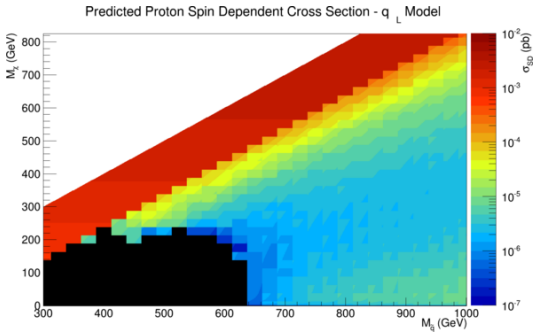

(c)

Figure 11. The predicted maximum spin-dependent proton-DM cross section from the combined Collider and Direct Detection bounds for Majorana Dark Matter.

JHEP01(2014)162

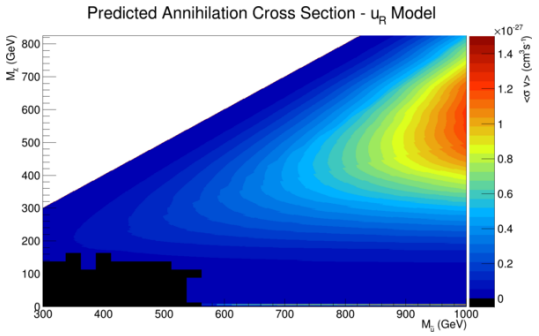

(a)

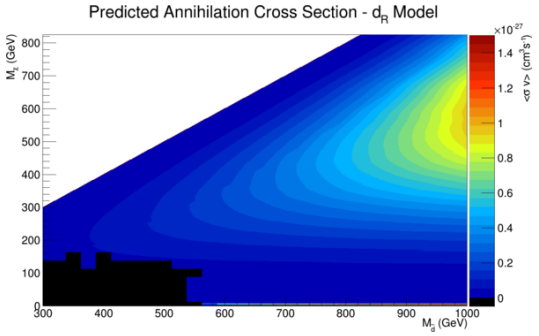

(b)

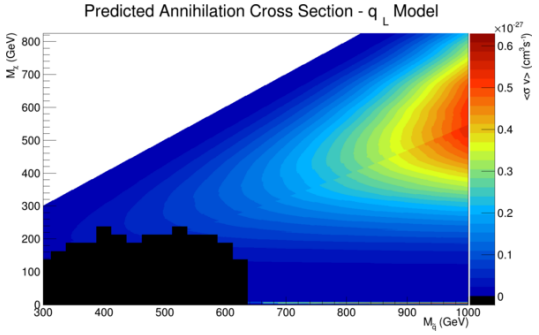

(c)

Figure 12. The predicted maximum annihilation cross section from the combined Collider and Direct Detection bounds for Dirac Dark Matter.

JHEP01(2014)162

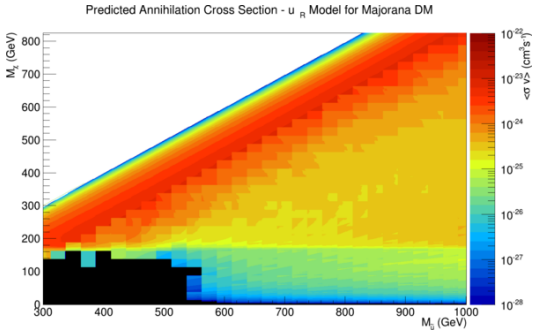

(a)

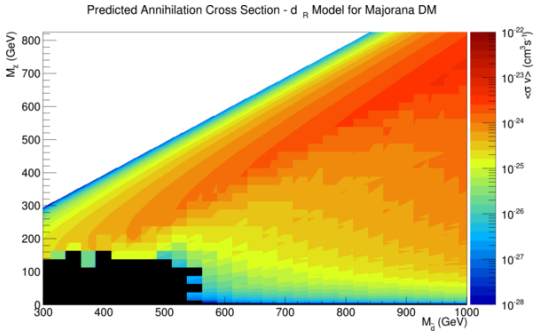

(b)

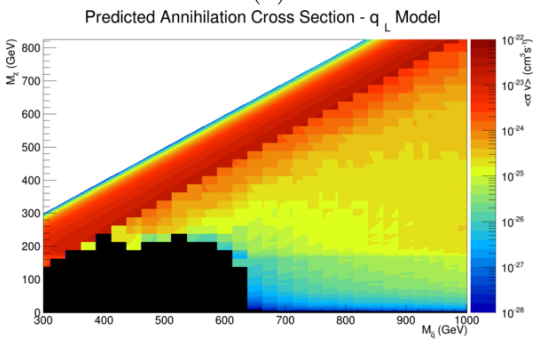

(c)

Figure 13. The predicted maximum annihilation cross section from the combined Collider and Direct Detection bounds for Majorana Dark Matter.

JHEP01(2014)162